



HAL
open science

Localization of brachytherapy seeds in TRUS images using rigid priors and medial forces

Vincent Jaouen, Julien Bert, Antoine Valeri, Dimitris Visvikis

► **To cite this version:**

Vincent Jaouen, Julien Bert, Antoine Valeri, Dimitris Visvikis. Localization of brachytherapy seeds in TRUS images using rigid priors and medial forces. *Surgetica* 2019, Jun 2019, Rennes, France. hal-02447809

HAL Id: hal-02447809

<https://hal.science/hal-02447809v1>

Submitted on 24 Jan 2020

HAL is a multi-disciplinary open access archive for the deposit and dissemination of scientific research documents, whether they are published or not. The documents may come from teaching and research institutions in France or abroad, or from public or private research centers.

L'archive ouverte pluridisciplinaire **HAL**, est destinée au dépôt et à la diffusion de documents scientifiques de niveau recherche, publiés ou non, émanant des établissements d'enseignement et de recherche français ou étrangers, des laboratoires publics ou privés.

Localization of brachytherapy seeds in TRUS images using rigid priors and medial forces

Vincent JAOUEN, Julien BERT, Antoine VALERI and Dimitris VISVIKIS

LaTIM-UMR 1101, Inserm, Brest University Hospital, University of Western Brittany, 29200 Brest, France

Contact: vincent.jouen@inserm.fr

We propose a new semi-automatic strategy for the localization of brachytherapy seeds with transrectal ultrasound imaging. We formulate the problem as a rigid surface-to-image registration, where a geometric model is embedded in an external force field pointing towards the last implanted seed. Considering the seed shape as a prior, we alleviate the need for *a posteriori* filtering among candidate shapes. Robustness to noise is enforced by constraining the model to rigid body motion and by privileging image intensity over higher order information. We present encouraging preliminary results on noisy synthetic images. More advanced validation on physical phantoms and clinical images is ongoing.

1 Introduction

Low-dose rate brachytherapy (LDR-B), one of the key treatment for prostate cancer, consists in inserting radioactive implants through the perineum directly into the prostate. The procedure is generally supervised under transrectal ultrasound (TRUS) guidance [1]. For every seed, potential errors may occur between expected and actual insertion site, advocating the recommendation for dynamic dose recalculation, where the configuration of the remaining seeds would ideally be updated using real time localization feedback [2]. In this context, one of the major difficulties of LDR-B lies in accurately localizing seeds directly from TRUS, a challenging task due to the inherent limitations of this modality [3][4][5].

In this paper, we propose a proof of concept for a seed localization technique based on evolving geometric

models. We embed a seed-like cylindrical model in an image-derived force field and constrain its evolution to rigid-body deformation, i.e. we only allow translations and rotations. The force field is computed so that it is oriented towards the medial axis of the nearest seed, providing fast and robust convergence towards the desired target. We successfully validate this concept on synthetic images. Validation on ultrasound imaging using physical phantoms and clinical data is ongoing.

2 Method

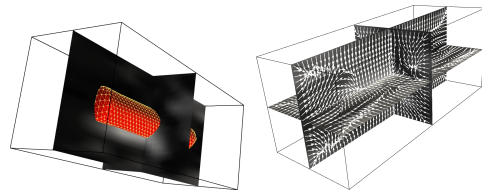


Figure 1: Search space I_i , initial model S^0 and orthogonal projections of the medial vector field \mathcal{F}_i (see text) for a real clinical case. Vectors are mostly oriented towards the medial axis of the seed.

The proposed localization workflow is as follows: 1) after each seed s_i is implanted, a cuboidal search space is defined in the vicinity of an initial position marked by the operator, reducing the image to a cropped region I_i (Fig. 1). 2) Then, a triangulated surface model S^t , where t is an artificial time variable, is rigidly evolved under an external force field \mathcal{F}_i associated with s_i , until it reaches steady state around the actual seed location. 3) The seed position is finally communicated to the treatment planning system to recalculate the dose plan accordingly.

One of our main contribution lies in the expression of the vector field \mathcal{F}_i associated with seed s_i . We exploit

This work was partly supported by the French ANR within the Investissements d'Avenir program (Labex CAMI) under reference ANR-11-LABX-0004 (Integrated project CAPRI)

a side property of external edge fields for deformable models such as Vector Field Convolution fields [6, 7] or gradient vector flow [8]: their ability to point towards the medial axis of objects if the intensity image itself is substituted for the edge map [9]. Rigid motion towards the medial axis can then be used to perform object segmentation, alleviating the need for higher order information (e.g. gradient or Hessian) typically employed in active contours frameworks [10, 11]. Such high order information would be unreliable in TRUS imaging due to excessive noise levels.

A Medial Vector Field [12] guiding the surface model is expressed as:

$$\mathcal{F}_i = I_i * \mathcal{K}, \quad (1)$$

where $*$ represents the convolution operation and:

$$\mathcal{K}(\mathbf{x}) = [K_x(x, y, z), K_y(x, y, z), K_z(x, y, z)] \quad (2)$$

is a vector field kernel (VFK), a vector kernel whose vectors point towards its center with decreasing magnitude [6]. To evolve the seed model, we first compute the motion of the set of free surface vertices \mathcal{V}_j of S^t embedded in the vector field \mathcal{F}_i :

$$\mathbf{V}^t = \mathbf{V}^{t-1} + \gamma \mathbf{F}, \quad (3)$$

where $\gamma < 1$ is a small artificial time step, \mathbf{V}^t is the coordinate matrix of vertices \mathcal{V}_j and \mathbf{F} is the force matrix corresponding to values of \mathcal{F}_i interpolated at \mathcal{V}_j . We then look for the rotation matrix \mathbf{R} and the translation vector \mathbf{T} closest to $\mathbf{V}^t - \mathbf{V}^{t-1}$ in the \mathcal{L}_2 sense:

$$\arg \min_{\mathbf{R}^t, \mathbf{T}^t} \frac{1}{N_v} \sum_{k=1}^{N_v} \|\mathbf{R}^t \cdot \mathbf{V}_k^{t-1} + \mathbf{T}^t - \mathbf{V}_k^t\|^2. \quad (4)$$

The solution of which is provided by singular value decomposition [13]. The rigid evolution of from S^{t-1} to S^t is then expressed as:

$$\mathbf{V}_R^t = \mathbf{V}^{t-1}[\mathbf{R}^t]^T + \mathbf{1}[\mathbf{T}^t]^T \quad (5)$$

where $\mathbf{1}$ is a vector composed only of ones.

The vertices coordinates \mathcal{V}_j of \mathcal{S} are then updated according to (5), and steps (3) to (5) are repeated until the surface converges to the location of seed s_i . The algorithm stops when the maximum displacement between two steps is less than a threshold value ϵ . These steps are performed after each implantation in almost real time, providing estimations of the orientation and localization of the last seed.

3 Results

We are currently at an early stage of the validation. As a proof of concept, we generated a synthetic 3D image showing pseudo seeds (PS) with different orientations, that we corrupted with heavy noise and Gaussian blur (Fig. 1). For each PS, we performed 50 initializations of

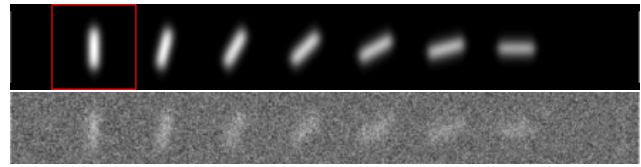


Figure 2: Axial slice of a synthetic 3D image showing seven seed-like patterns with various orientations. Top: clean image. Bottom: noisy image.

the model by uniformly drawing initial coordinates in a $25 \times 25 \times 5$ voxels neighborhood window (red square, Fig. 1). Distance (in voxels) between true and estimated barycenters and angular error between the PS and the surface model (obtained through principal component analysis) were used as quantitative metrics [4], and are shown in Fig. 3. Results are encouraging given the low signal-to-noise ratio of the image, with errors of a few voxels and orientation estimations generally less than ten degrees off, with rare failure cases. A physical phantom for ultrasound is also currently studied for which preliminary, unquantified results are presented in Fig. 4. Results on real TRUS images using expert consensus are also considered for a thorough validation of the approach.

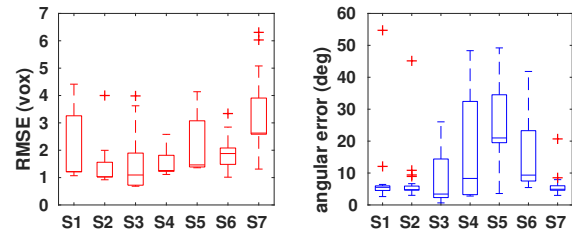


Figure 3: Barycenter distance and angular error for the 7 pseudo seeds using multiple initializations

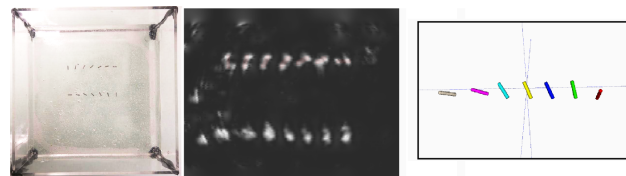


Figure 4: Left: physical seed phantom. Middle: US image. Right: preliminary unquantified localization results corresponding to the bottom row.

4 Conclusion

We have presented a proof of concept for a fast semi-automatic seed localization method using rigid geometric models, where the seed shape is incorporated as a prior. Early results on synthetic images support the potential interest of the approach for real time, intraoperative seed localization for dynamic dose estimation.

References

- [1] S. Nag, D. Beyer, J. Friedland, P. Grimm, and R. Nath, “American Brachytherapy Society (ABS) recommendations for transperineal permanent brachytherapy of prostate cancer,” *International Journal of Radiation Oncology* Biology* Physics*, vol. 44, no. 4, pp. 789–799, 1999.
- [2] A. Polo, C. Salembier, J. Venselaar, P. Hoskin, P. group of the GEC ESTRO, *et al.*, “Review of intraoperative imaging and planning techniques in permanent seed prostate brachytherapy,” *Radiotherapy and Oncology*, vol. 94, no. 1, pp. 12–23, 2010.
- [3] B. H. Han, K. Wallner, G. Merrick, W. Butler, S. Sutlief, and J. Sylvester, “Prostate brachytherapy seed identification on post-implant TRUS images,” *Medical physics*, vol. 30, no. 5, pp. 898–900, 2003.
- [4] Z. Wei, L. Gardi, D. B. Downey, and A. Fenster, “Automated localization of implanted seeds in 3D TRUS images used for prostate brachytherapy,” *Medical physics*, vol. 33, no. 7Part1, pp. 2404–2417, 2006.
- [5] X. Wen, S. E. Salcudean, and P. D. Lawrence, “Detection of brachytherapy seeds using 3-D transrectal ultrasound,” *IEEE Transactions on Biomedical Engineering*, vol. 57, no. 10, pp. 2467–2477, 2010.
- [6] B. Li and S. T. Acton, “Active contour external force using vector field convolution for image segmentation,” *IEEE Transactions on Image Processing*, vol. 16, no. 8, pp. 2096–2106, 2007.
- [7] V. Jaouen, J. Bert, N. Boussion, H. Fayad, M. Hatt, and D. Visvikis, “Image enhancement with PDEs and nonconservative advection flow fields,” *IEEE Transactions on Image Processing*, vol. DOI: 10.1109/TIP.2018.2881838, 2018.
- [8] C. Xu, J. L. Prince, *et al.*, “Snakes, shapes, and gradient vector flow,” *IEEE Transactions on Image Processing*, vol. 7, no. 3, pp. 359–369, 1998.
- [9] S. Mukherjee and S. T. Acton, “Vector field convolution medialness applied to neuron tracing,” in *2013 IEEE International Conference on Image Processing*, pp. 665–669, IEEE, 2013.
- [10] B. Li, S. A. Millington, D. D. Anderson, and S. T. Acton, “Registration of surfaces to 3D images using rigid body surfaces,” in *2006 Fortieth Asilomar Conference on Signals, Systems and Computers*, pp. 416–420, IEEE, 2006.
- [11] V. Jaouen, P. Gonzalez, S. Stute, D. Guilloteau, S. Chalon, I. Buvat, and C. Tauber, “Variational segmentation of vector-valued images with gradient vector flow,” *IEEE Transactions on Image Processing*, vol. 23, no. 11, pp. 4773–4785, 2014.
- [12] V. Jaouen, J. Bert, I. Hamdan, A. Valéri, U. Schick, N. Boussion, and D. Visvikis, “Purely edge-based prostate segmentation in 3D TRUS images using deformable models,” in *Surgetica 2017*, 2017.
- [13] K. S. Arun, T. S. Huang, and S. D. Blostein, “Least-squares fitting of two 3-D point sets,” *IEEE Transactions on Pattern Analysis and Machine Intelligence*, no. 5, pp. 698–700, 1987.